Title: Magnetic fields in the early universe and beam-plasma instabilities

Date: Mar 15, 2016 09:45 AM

URL: http://pirsa.org/16030098

Abstract:

Datei Bearbeiten Suche Ansicht Textsatz Scripts Fenster Hilfe

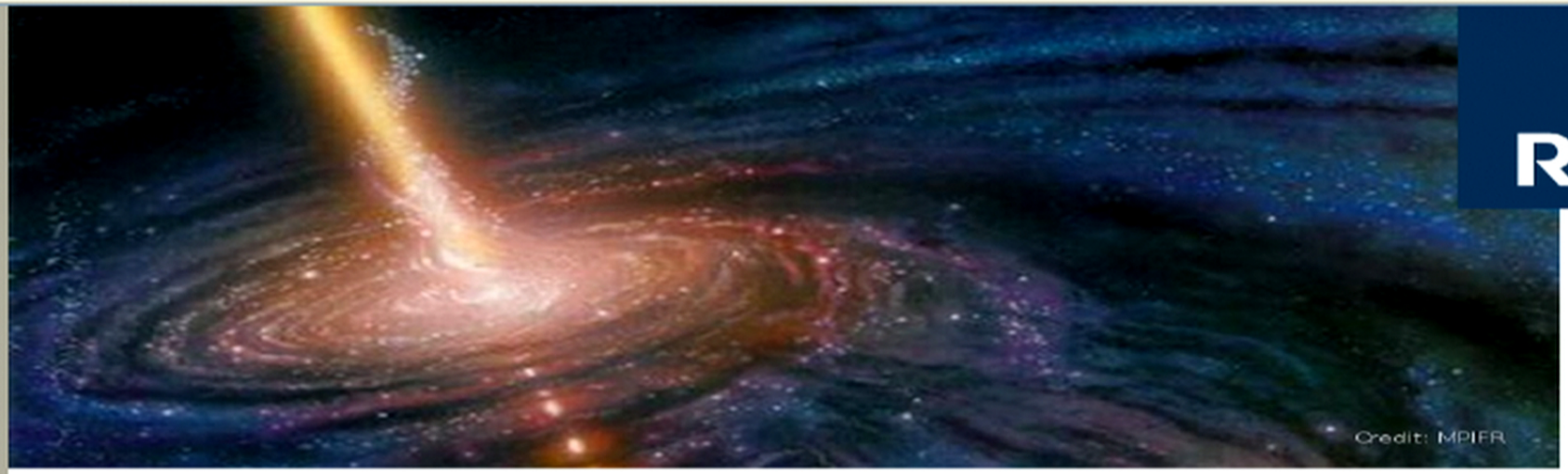

RUB

RUHR-UNIVERSITÄT BOCHUM

Magnetic fields in the early universe and beam-plasma instabilities

Reinhard Schlickeiser
Institut für Theoretische Physik IV: Weltraum- und Astrophysik, Ruhr-Universität Bochum, Germany

Waterloo 2016-03-15

RUHR-UNIVERSITÄT BOCHUM
Theoretische Physik IV: Weltraum- und Astrophysik

RUB

Collaborators and topics

Collaborators: Tim Felten, Ulrich Kolberg, Steffen Krakau, Ulf Menzler (RUB), Peter H. Yoon (University of Maryland)

Topics:

1. Introduction
2. Upper bounds on the EGMF
3. Lower EGMF bounds from γ-ray astronomy?
4. Lower bounds from fluctuation theory
5. From disordered to ordered magnetic field structures
6. Summary and conclusions

RUHR-UNIVERSITÄT BOCHUM
Theoretische Physik IV: Weltraum- und Astrophysik

RUB

Origin of cosmic magnetic fields

Many astrophysicists believe that galactic and extragalactic magnetic fields (EGMF) are generated and maintained by dynamo action, whereby the energy associated with e.g. the differential rotation of spiral galaxies is converted into magnetic field energy.

However, the dynamo mechanism is only a means of amplification, and dynamos require finite **seed magnetic fields**. These seed fields are needed for possible instabilities from anisotropic plasma particle distribution functions, MHD instabilities (such as the magneto-rotational instability), kinetic plasma instabilities (such as the Weibel and filamentation instabilities (RS and Shukla 2003)) and/or the MHD dynamo process (e.g. Schober, Banerjee, Klessen et al. 2015), which grow according to $d(\delta B)^2/dt = 2\gamma(\delta B)^2$, so that

$$(\delta B)^2(t) = (\delta B)^2(t=0)e^{2\gamma t} \qquad (1)$$

RUHR-UNIVERSITÄT BOCHUM
Theoretische Physik IV: Weltraum- und Astrophysik

RUB

Origin of cosmic magnetic fields (2)

Obviously, a nonvanishing initial $(\delta B)^2(t=0) \neq 0$ **seed magnetic field** energy density is required. Neither the dynamo process nor plasma instabilities generate magnetic fields without such seed fields.

Permanent ferromagnetism cannot operate in the early universe as it is a property of only a few densely packed materials, such as iron, in which the spin exchange interactions of individual atoms naturally line up in the same direction and create a residual persistent magnetic field. In the early universe, before iron and other magnetic materials had been created inside stars, such permanent magnetism did not exist.

Upper bounds on the EGMF

Contrary to magnetic fields in galaxies and galaxy clusters, EGMF in the intergalactic medium (IGM) have not been detected sofar (Neronov and Semikoz 2009). Only upper limits exist, which are shown in Fig. 1.

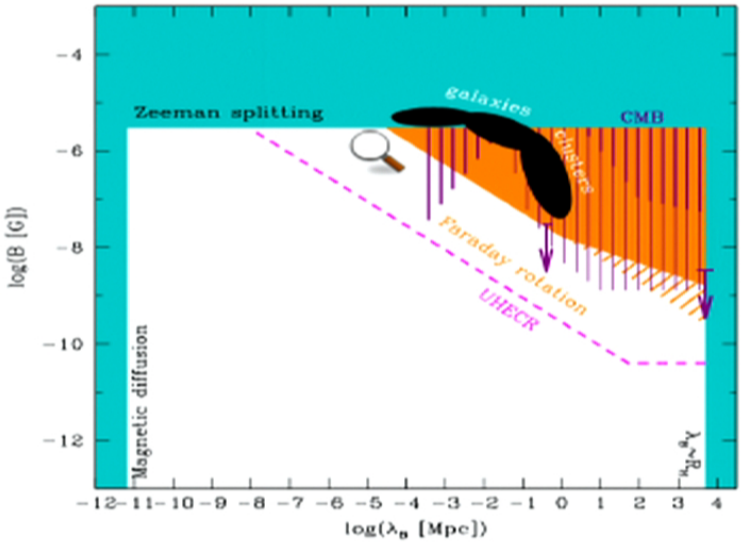

Figure 1: Present-day (redshift $z = 0$) observational upper limits on EGMF (from Neronov and Semikoz (2009, PRD 80, 123012).

RUHR-UNIVERSITÄT BOCHUM
Theoretische Physik IV: Weltraum- und Astrophysik

RUB

Lower EGMF bounds from γ-ray astronomy?

Neronov and Vovk (2010) have argued that lower bounds (shown in Fig. 2) on the EGMF can be derived from GeV-TeV detected blazars at cosmological distances.

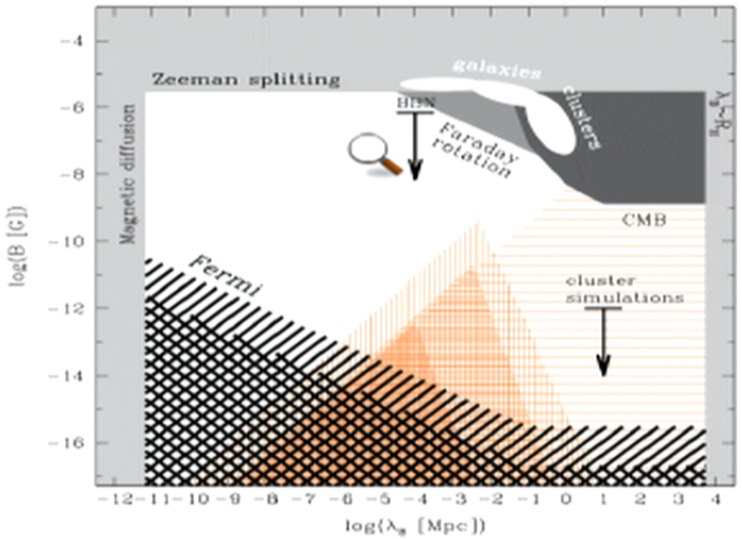

Figure 2: Observational bounds on EGMF (from Neronov and Vovk (2010, Science 328, 73).

RUHR-UNIVERSITÄT BOCHUM
Theoretische Physik IV: Weltraum- und Astrophysik

RUB

Lower EGMF bounds from γ-rays (2)

The new generation of air Cherenkov TeV γ-ray telescopes (HESS, MAGIC, VERITAS) have detected about 30 cosmological blazars with strong TeV photon emission (see e.g. Fig. 3). The most distant ones are PKS 1441+25 (redshift $z = 0.939$), the gravitationally lensed blazar QSO B0218+357 ($z = 0.944$), 3C279 (redshift $z = 0.536$), 3C66A ($z = 0.444$), PKS 1510-089 ($z = 0.361$) and 1ES 0412+009 ($z = 0.287$).

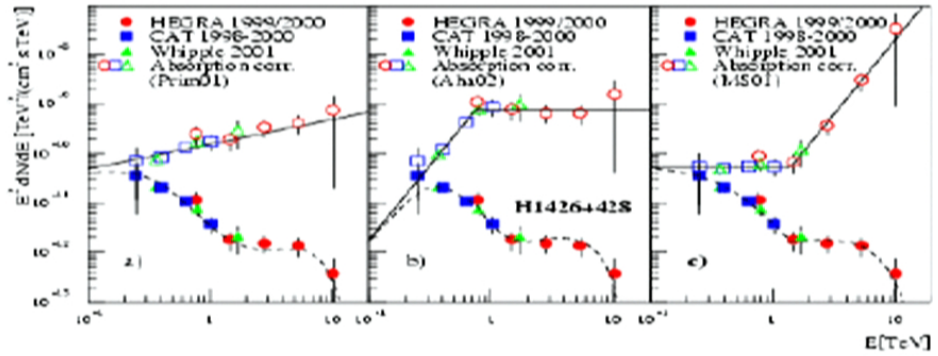

Figure 3: High-energy photon spectrum from blazar H1426+428

RUHR-UNIVERSITÄT BOCHUM
Theoretische Physik IV: Weltraum- und Astrophysik

RUB

Lower EGMF bounds from γ-rays (3)

Any of these more distant than $z = 0.018$ produces energetic $e^{\pm}$ particle beams in double photon collisions $\gamma(\mathrm{TeV}) + \gamma(\mathrm{EBL}) \rightarrow e^{+} + e^{-}$ with the extragalactic background light (EBL) once $E_\gamma \geq m_e^2 c^4 / E_{\mathrm{EBL}}$: see Fig. 4.

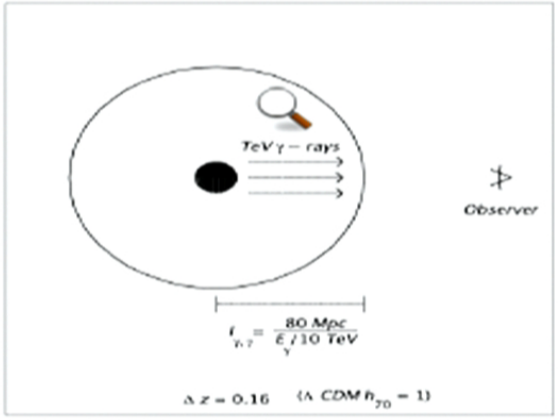

Figure 4: Intergalactic pair beam production: TeV photons from any blazar more distant away than $z = 0.018$ produce relativistic pairs by double photon collisions with the EBL soft photons.

RUHR-UNIVERSITÄT BOCHUM
Theoretische Physik IV: Weltraum- und Astrophysik

RUB

Lower EGMF bounds from γ-rays (4)

These pairs with typical Lorentz factors $10^6\Gamma_6$ are expected to inverse Compton (IC) scatter on the cosmic microwave background (CMB) radiation, on a typical length scale $l_{IC} \sim 0.75\Gamma_6^{-1}$ Mpc (corresponding time scale $t_{IC} = l_{IC}/c = 2.5 \cdot 10^6\Gamma_6^{-1}$ yrs), producing gamma-rays with energy of order 100 GeV. These inverse Compton gamma-rays then are still energetic enough for further pair-production interactions giving rise to a full electromagnetic cascade as in vacuum.

But these inverse Compton gamma rays have **not** been detected by the FERMI satellite! Neronov and Vovk (2010) explained this non-detection by strong enough stochastic EGMF which scatter the produced pairs, so that the inverse Compton gamma rays are misdirected from the blazar direction.

RUHR-UNIVERSITÄT BOCHUM
Theoretische Physik IV: Weltraum- und Astrophysik

RUB

Lower EGMF bounds from γ-rays (5)

However, Pfrommer et al. (2013) noted that the emission from all unresolved blazars overproduces the observed extragalactic gamma-ray background at GeV energies. The magnetic deflection processes of pairs and their inverse Compton emission out of our line-of-sight is on average balanced by deflecting other pairs and their inverse Compton emission into our line-of-sight, so that the resulting isotropic extragalactic gamma-ray background remains invariant.

A solution to this vacuum cascade overproduction problem, which also would invalidate the lower bounds of the EGMF by Neronov and Vovk (2010), is offered by accounting for the plasma effects of the relativistic pairs generated in the first double photon interaction with the production spectrum shown in Fig. 5.

RUHR-UNIVERSITÄT BOCHUM
Theoretische Physik IV: Weltraum- und Astrophysik

RUB

Lower EGMF bounds from γ-rays (6)

Using linear reactive and kinetic instability analysis Broderick, Chang and Pfrommer (2012) and RS et al. (2012) have shown that the created pair beam distribution function is quickly unstable (on time scales $t_E \ll t_{IC}$).

The quasilinear backreaction of the excited electrostatic oscillations then relaxes (on time sales $\simeq 100 t_E$) the initial distribution to the "plateau" distribution with $(\partial f/\partial \epsilon) = 0$ (see Fig. 6), which has only ≤ 50 percent total energy compared to the initial distribution (the other 50 percent are transferred to the electrostatic oscillations).

Hence the generation of inverse-Compton scattered GeV gamma-ray photons by the pair beam is significantly (by a factor 10 for full plateauing) suppressed. Less kinetic pair energy is available for inverse Compton interactions with the CMB (Menzler and RS 2015), in agreement with the FERMI observations, see Fig. 7.

RUHR-UNIVERSITÄT BOCHUM
Theoretische Physik IV: Weltraum- und Astrophysik

RUB

Lower EGMF bounds from γ-rays (5)

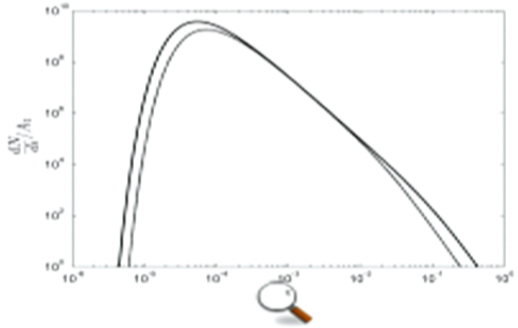

Figure 5: Differential pair production spectrum as a function of $\epsilon = 2p_{||}\,c/10^{10}\,m_e c^2$ from a power-law distributed gamma-ray beam. From RS, A. Elyiv, D. Ibscher and F. Miniati (2012).

Because of the strong energy inversion $(\partial f/\partial\epsilon) > 0$ of the corresponding phase space density $f(\epsilon) = \epsilon^{-2}(dN/d\epsilon)$ below the maximum, this initially generated pair-beam distribution function is subject to two-stream-like instabilities of both electrostatic and electromagnetic nature in the unmagnetized, fully-ionized IGM (additional induced emission as in masers).

RUHR-UNIVERSITÄT BOCHUM
Theoretische Physik IV: Weltraum- und Astrophysik

RUB

Lower EGMF bounds from γ-rays (7)

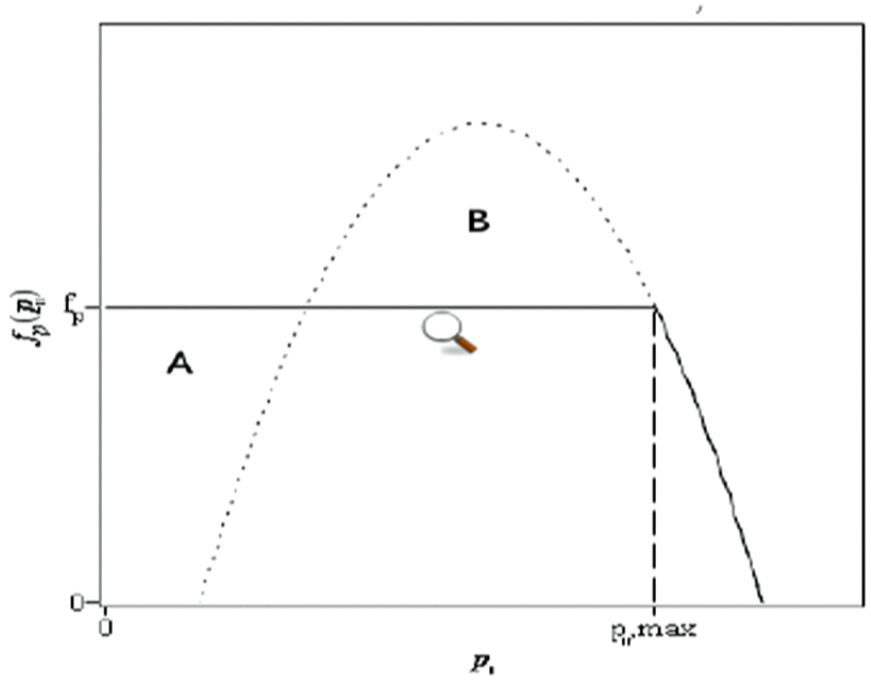

Figure 6: Geometrical representation of the plateauing effect in $p_\parallel$. The dotted line represents an illustrative initial pair spectrum. The solid line shows the final spectrum. Particle number conservation requires the areas A and B to be equal.

RUHR-UNIVERSITÄT BOCHUM
Theoretische Physik IV: Weltraum- und Astrophysik

RUB

Lower EGMF bounds from γ-rays (8)

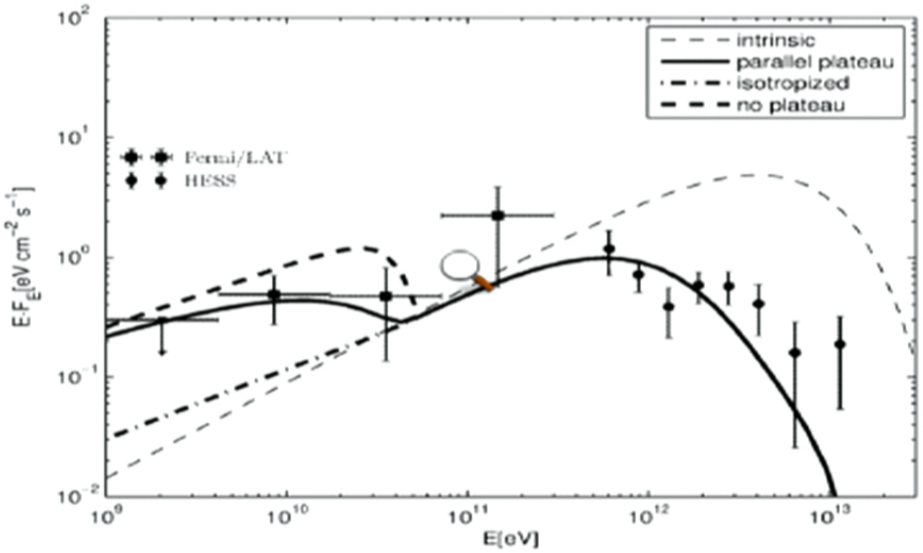

Figure 7: GeV-Tex emission from plateaued and non-plateaued pair distribution functions compared with the observations of the blazar 1ES 0229+200. From Menzler and RS (2015).

RUHR-UNIVERSITÄT BOCHUM
Theoretische Physik IV: Weltraum- und Astrophysik

RUB

Lower EGMF bounds from γ-rays (9)

The generated electrostatic oscillation energy heats the IGM with important consequences for its thermal history (Chang et al. 2012) and the formation of cosmic structures.

Most importantly: there is no need to require the existence of small intergalactic magnetic fields, to scatter the produced pairs away from the line of sight, in order to explain the FERMI non-detection of the inverse Compton scattered GeV gamma rays. In particular, the various derived lower bounds for the EGMF in Fig. 2 need to be modified due to the pair beam instability argument, although we do not question the principal existence of turbulent intergalactic magnetic fields.

More work needed on: partial versus full plateauing, nonlinear beam stabilization processes, role of small but finite spread in perpendicular momentum of pair production spectrum (Miniati and Elyiv 2013), influence of excited transverse oscillations (see below).

RUHR-UNIVERSITÄT BOCHUM
Theoretische Physik IV: Weltraum- und Astrophysik

RUB

Lower bounds from plasma fluctuation theory

Before the formation of the first stars but after the reionization at $z \simeq 20$, the luminous intergalactic matter consisted only of a fully ionised gas of protons, electrons, helium nuclei and lithium nuclei which were produced during the Big Bang. The physical parameters that describe the state of this gas are, however, not constant. Density and pressure fluctuate around certain mean values, and consequently electric and magnetic fields fluctuate around vanishing mean values, due to the thermal motion of the plasma particles. This small but finite dispersion in the form of random magnetic fields has now been calculated with kinetic plasma fluctuation theory.

The fluctuations are descibed by real wave vectors ($\vec{k}$) and complex frequencies $\omega(\vec{k}) = \omega_R(\vec{k}) + \imath\gamma(\vec{k})$, implying for the space- and time-dependence of e.g. magnetic fluctuations the superposition of

$$\delta\vec{B}(\vec{x}, t) \propto \exp[\imath(\vec{k} \cdot \vec{x} - \omega_R t) + \gamma t] \qquad (2)$$

RUHR-UNIVERSITÄT BOCHUM
Theoretische Physik IV: Weltraum- und Astrophysik

RUB

Plasma fluctuations

One distinguishes between

- **collective** modes with a fixed dispersion relation $\omega = \omega(\vec{k})$, e.g. electromagnetic waves in vacuum $\omega_R^2 = c^2 k^2$ and $\gamma = 0$,
- **non-collective** modes with no dispersion relation $\omega = \omega(\vec{k})$, and, regarding the real (ω_R) and imaginary (γ) part of the frequency,
- **weakly damped/amplified** wave-like modes with $|\gamma| \ll |\omega_R|$
- **weakly propagating** modes with $|\omega_R| \ll |\gamma|$, including **aperiodic** fluctuations ($\omega_R = 0$). Aperiodic oscillations fluctuate only in space, do not propagate as $\omega_R = 0$, but permanently grow or decrease in time depending on the sign of γ.

As in-situ plasma turbulence observations have shown the interplanetary medium is full with aperiodic fluctuations in the form of mirror, firehose and ordinary mode oscillations, so that there is no doubt that they exist in nature!

RUB

Weakly amplified/damped oscillations

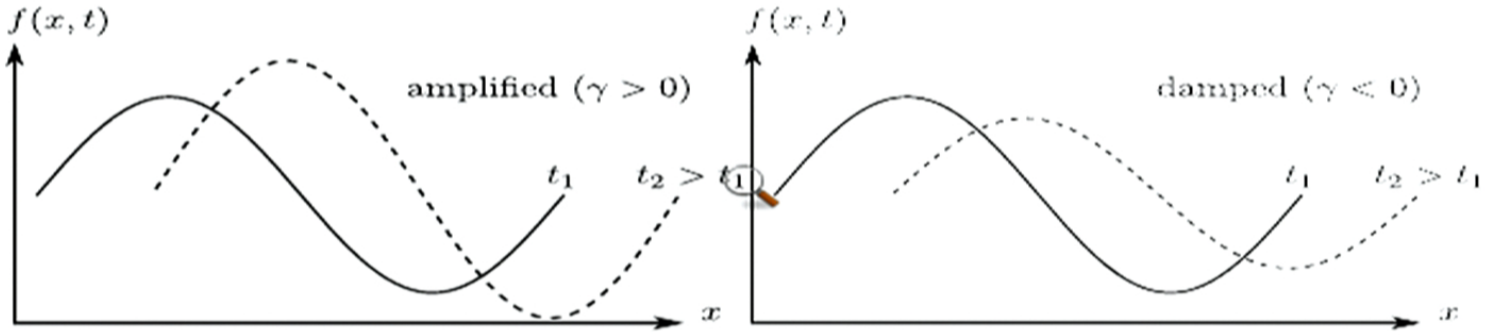

Figure 8: Sketch of weakly amplified ($\gamma > 0$, left) and weakly damped ($\gamma < 0$, right) monochromatic plasma wave ($\omega_R \gg |\gamma|$).

RUB

Weakly propagating amplified/damped oscillations

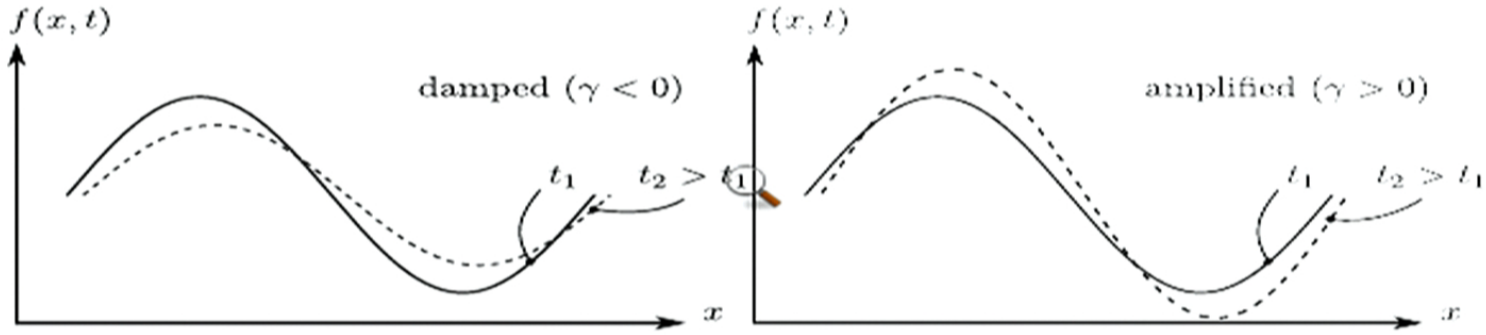

Figure 9: Sketch of weakly propagating damped ($\gamma < 0$, left) and weakly propagating amplified ($\gamma < 0$, right) monochromatic fluctuation ($\omega_R \ll |\gamma|$).

RUB

Weakly aperiodic oscillations

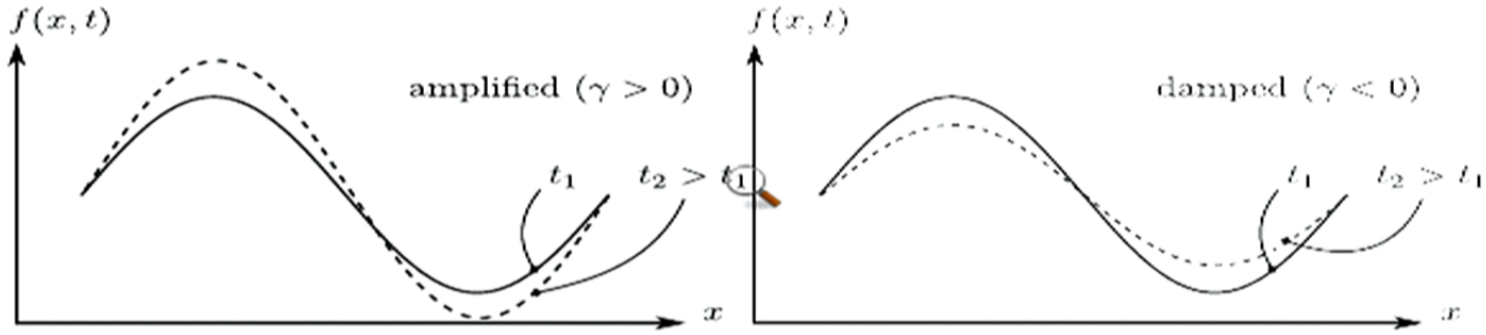

Figure 10: Sketch of aperiodic ($\omega_R = 0$) growing ($\gamma > 0$, left) and aperiodic damped ($\gamma < 0$, right) monochromatic fluctuation.

RUHR-UNIVERSITÄT BOCHUM
Theoretische Physik IV: Weltraum- und Astrophysik

RUB

Fluctuation-dissipation theorem

Unlike for weakly amplified/damped modes (Salpeter 1960, Sitenko 1967, Ichimaru 1973, Kegel 1998) only recently general expressions for the electromagnetic fluctuation spectra from uncorrelated plasma particles in unmagnetized (RS and Yoon 2012) and magnetized (RS and Yoon 2015) plasmas for arbitrary frequencies have been derived using the system of the Klimontovich and Maxwell equations.

In the IGM the fluctuation spectra can be calculated from the fluctuation-dissipation theorem (FDT) in plasmas holding for isotropic equal-temperature thermal plasmas. For non-collective transverse oscillations with arbitrary complex frequencies $\omega = \omega_R + \imath\gamma$ the FDT in unmagnetized plasmas reads (RS and Kolberg 2015)

$$< (\delta B)^2 > (k,\omega) = -\frac{4k_B T_0 k^2 c^2 \sigma}{(2\pi)^3 |\omega|^2} \Im\left(\frac{1}{\omega}\left[\frac{1}{\Lambda_T} - \frac{1+\frac{k^2c^2}{|\omega|^2}}{|\Lambda_T|^2}\right]\right) \qquad (3)$$

in terms of the thermal transverse dispersion function $\Lambda_T(k,\omega)$.

RUHR-UNIVERSITÄT BOCHUM
Theoretische Physik IV: Weltraum- und Astrophysik

RUB

Thermal aperiodic noise in the IGM

The present IGM has temperatures of about $T_0 = 10^4\, T_4 \mathrm{K}$ and ionized gas densities of $n_e = 10^{-7} n_{-7}$ cm^{-3}. The spontaneously emitted aperiodic transverse magnetic field fluctuation spectrum over the whole complex frequency calculated from Eq. (3) is shown in Fig. 11. Obviously, it is dominated by a damped mode with negative values of γ.

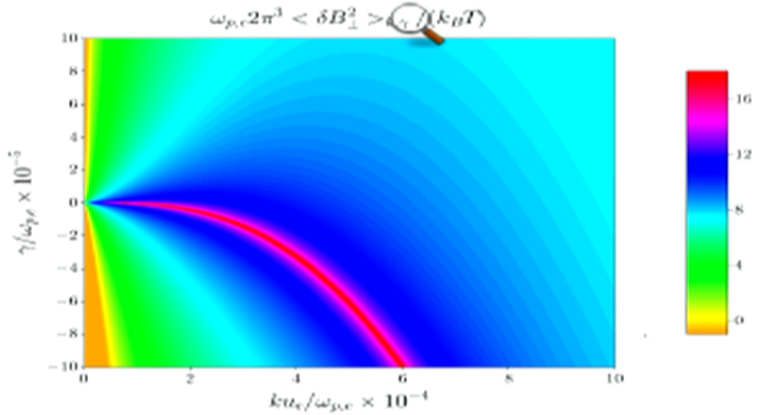

Figure 11: Spontaneously emitted thermal aperiodic magnetic noise in the IGM in units of $k_B T_e/(2\pi^3 \omega_{p,e})$. The colour scale is logarithmic in powers of e. From Felten et al. (2013).

RUHR-UNIVERSITÄT BOCHUM
Theoretische Physik IV: Weltraum- und Astrophysik

RUB

Thermal aperiodic noise in the IGM (2)

Integrating over all frequencies γ provides the equilibrium thermal electric and magnetic field wavenumber fluctuation spectra shown in Fig. 12. The magnetic fluctuation spectrum is not of Kolmogorov form! It holds for maximum spatial magnetic turbulence scales of

$$\lambda < \lambda_{\max} = 2.4 \cdot 10^{15}\, T_4^{1/6}\, n_{-7}^{-1/3} \text{ cm} = 7.7 \cdot 10^{-10}\, T_4^{1/6}\, n_{-7}^{-1/3} \text{ Mpc}.$$

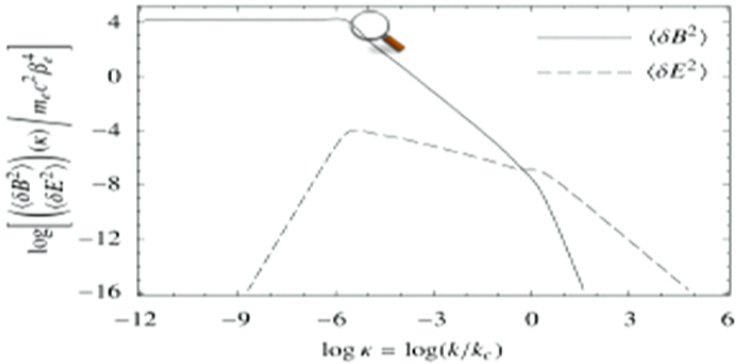

Figure 12: Thermal wavenumber spectra of electric (dashed curve) and magnetic (full curve) field fluctuations in units of $m_e c^2 \beta_e^4$ in an electron-proton plasma calculated for the plasma temperature $T_0 = 10^4\, T_4$ K. From Yoon, RS and Kolberg (2014).

RUHR-UNIVERSITÄT BOCHUM
Theoretische Physik IV: Weltraum- und Astrophysik

RUB

Total strength of fluctuating magnetic field

By integrating the wavenumber fluctuation spectrum over all wavenumber values we find for the total magnetic field strength at $z = 0$

$$|\delta B(z=0)| = \sqrt{(\delta B)^2(z=0)} = 6.3 \cdot 10^{-18}\, n_{-7}^{3/4}\, T_4^{1/8}\ \mathrm{G}, \qquad (4)$$

With $n_{-7}(z) = n_{-7}(1+z)^3$ and $T_4(z) = T_4(1+z)$ we obtain at the onset of reionization ($z = 20$)

$$|\delta B(z=20)| = 8.7 \cdot 10^{-15}\ \mathrm{G} \qquad (5)$$

This guaranteed EGMF in the form of randomly distributed aperiodic oscillations with volume filling factor $\mathcal{V} \simeq 1$, produced by the spontaneous emission of the isotropic thermal IGM plasma, serves as seed fields for possible amplification by later possible plasma instabilities from anisotropic plasma particle distribution functions, MHD instabilities and/or the MHD dynamo process (RS 2012).

RUHR-UNIVERSITÄT BOCHUM
Theoretische Physik IV: Weltraum- und Astrophysik

RUB

Total strength of fluctuating magnetic field (2)

The strength of the guaranteed spontaneously emitted magnetic seed fields (5) is orders of magnitude larger than the seed fields from the Biermann (1950) battery process (10^{-18} G) with tiny volume filling factor and cosmological phase transitions (Sigl et al. 1997) (10^{-20} G).

These spontaneously emitted fluctuations have typical plasma scale lengths $2.4 \cdot 10^{15}(1+z)^{-5/6}$ cm, but as argued below, the first hydrodynamical compression generates considerably longer correlation lengths of the compressed magnetic fields determined by the spatial scale of the compressor (see Fig. 13).

RUHR-UNIVERSITÄT BOCHUM
Theoretische Physik IV: Weltraum- und Astrophysik

RUB

From disordered to ordered magnetic field structures

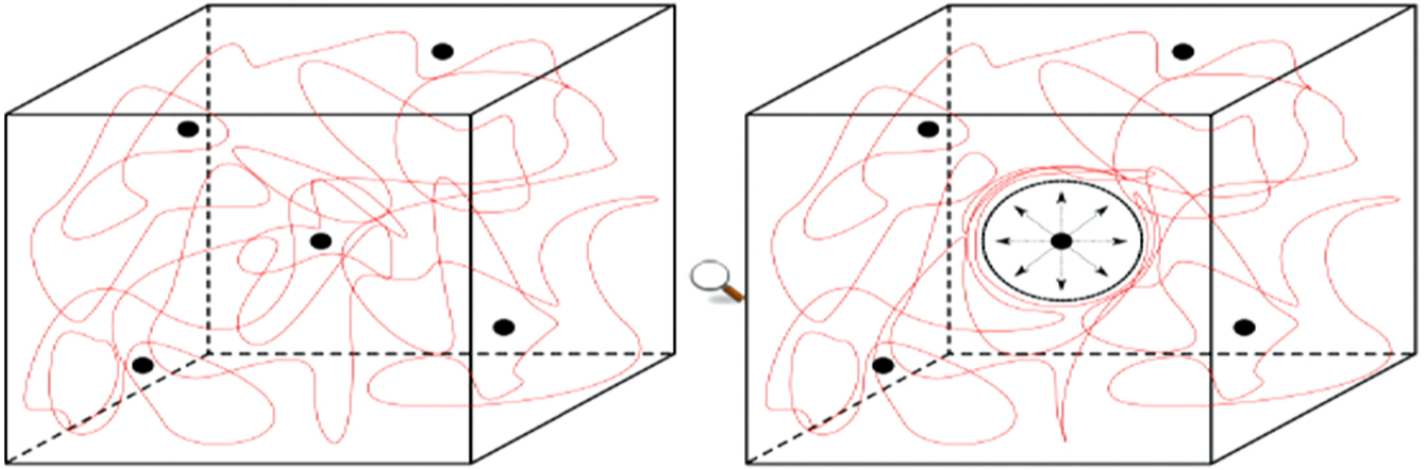

Figure 13: Illustration of the hydrodynamical stretching and ordering of cosmic magnetic fields. On the left figure a turbulent random magnetic field pervades the medium between five protostars. The right figure shows the ordering and stretching of the magnetic field as one of the stars explodes as a supernova. The outgoing shock wave compresses and orders the magnetic field in its vicinity. From RS and Yoon (2015).

RUHR-UNIVERSITÄT BOCHUM
Theoretische Physik IV: Weltraum- und Astrophysik

RUB

To ordered magnetic field structures (2)

The unmagnetized, isotropic, thermal and steady IGM plasma by spontaneous emission generates steady tangled fields, isotropically distributed in direction, on small spatial scales $\leq 10^{15}$ cm. Because of its ultrahigh turbulent plasma beta value ($\beta_t = 10^{17}\, n_{-7}^{-1/2}\, T_4^{3/4}$), these seed fields are too weak to affect the dynamics of the IGM plasma, but are tied passively to the highly conducting IGM plasma as frozen-in magnetic fluxes.

Earlier analytical considerations and numerical simulations (Laing 1980, Hughes et al. 1985, Matthews and Scheuer 1990) showed that any shear and/or compression of the IGM medium enormously amplify these seed magnetic fields and make them anisotropic. Depending on the specific exerted compression and/or shear, even one-dimensional ordered magnetic field structures can be generated out of the original isotropically tangled field configuration.

RUHR-UNIVERSITÄT BOCHUM
Theoretische Physik IV: Weltraum- und Astrophysik

RUB

To ordered magnetic field structures (3)

Hydrodynamical compression or shearing of the IGM medium arises from the shock waves of the supernova explosions of the first stars at the end of their lifetime, or from supersonic stellar and galactic winds. Fig. 13 sketches the basic physical process.

Obviously, this magnetic field stretching and ordering occurs only in gas regions overrun frequently by shocks and winds. Each individual shock or wind (with speed V_s) compression orders the field on spatial scales R on time scales given by the short shock crossing time R/V_s, but signifant amplification requires multiple compressions. The ordered magnetic field filling factor is determined by the shock's and wind's filling factors which are large (80 percent) in the coronal phase of interstellar media (McKee and Ostriker 1977) and near shock waves in large-scale cosmic structures (Miniati et al. 2000).

RUHR-UNIVERSITÄT BOCHUM
Theoretische Physik IV: Weltraum- und Astrophysik

RUB

To ordered magnetic field structures (3)

Hydrodynamical compression or shearing of the IGM medium arises from the shock waves of the supernova explosions of the first stars at the end of their lifetime, or from supersonic stellar and galactic winds. Fig. 13 sketches the basic physical process.

Obviously, this magnetic field stretching and ordering occurs only in gas regions overrun frequently by shocks and winds. Each individual shock or wind (with speed V_s) compression orders the field on spatial scales R on time scales given by the short shock crossing time R/V_s, but signifant amplification requires multiple compressions. The ordered magnetic field filling factor is determined by the shock's and wind's filling factors which are large (80 percent) in the coronal phase of interstellar media (McKee and Ostriker 1977) and near shock waves in large-scale cosmic structures (Miniati et al. 2000).

RUHR-UNIVERSITÄT BOCHUM
Theoretische Physik IV: Weltraum- und Astrophysik

RUB

Summary and conclusions

- Contrary to magnetic fields in galaxies and galaxy clusters, extragalactic magnetic fields (EGMF) in the intergalactic medium (IGM) have not been detected sofar. We reviewed the upper and lower bounds on the strength and correlation length of the EGMF.
- The lower bounds from γ-ray astronomy need to be modified due to the pair beam instability argument which offers a different explanation of the FERMI non-detection of inverse Compton gamma rays from cascaded TeV emission of distant blazars.
- A lower bound of $|\delta B(z = 20)| = 8.7 \cdot 10^{-15}$ G at scales $\lambda < 6 \cdot 10^{-11}$ Mpc is set by plasma fluctuation theory, because the unmagnetized fully-ionized thermal IGM plasma emits transverse aperiodic fluctuations.
- The stochastic magnetic fields serve well as cosmological seed fields for further amplification processes once additional kinetic free energy becomes available in these plasmas (a new primary dynamo process).

RUHR-UNIVERSITÄT BOCHUM
Theoretische Physik IV: Weltraum- und Astrophysik

RUB

Summary and conclusions (2)

- The shear and/or compression of the intergalactic medium exerted by the first supernova explosions amplify these seed fields and make them anisotropic, until the magnetic restoring forces affect the gas dynamics.
- Financial support by the Deutsche Forschungsgemeinschaft is gratefully acknowledged.

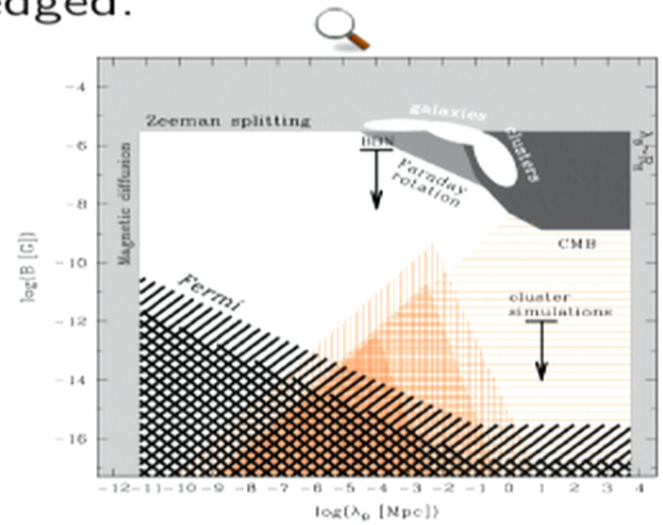

RUHR-UNIVERSITÄT BOCHUM
Theoretische Physik IV: Weltraum- und Astrophysik

RUB

Pair beam saturation in the IGM: more details

(for details see RS et al., A& A 393, 69 (2002)) Neglecting spatial dependencies, the time-dependent behaviour of the intensities of the excited electrostatic waves is determined by the weak turbulence kinetic equation

$$\frac{\partial I_e(k,t)}{\partial t} = 2\psi_e(k,t) I_e(k,t) + S_e(k) - \psi_{\rm LD}(k) I_e(k,t) - \sum_i d_i I_e(k,t) I_i(k,t), \quad (6)$$

where the red terms refer to the quasilinear evolution. The nonred terms describe the steady spontaneous emission coefficient (S_e), the Landau damping ($\psi_{\rm LD}(k)$) of electrostatic waves by the thermal IGM $e-p$-plasma and the nonlinear wave-wave interactions with other eigenmodes (e. g. ion sound waves, transverse filamentation and Weibel modes. . .) of intensity $I_i(k,t)$), including nonlinear Landau damping when $i = e$. The other eigenmodes obey similar kinetic equations.

RUHR-UNIVERSITÄT BOCHUM
Theoretische Physik IV: Weltraum- und Astrophysik

RUB

Pair beam saturation in the IGM: more details

(for details see RS et al., A& A 393, 69 (2002)) Neglecting spatial dependencies, the time-dependent behaviour of the intensities of the excited electrostatic waves is determined by the weak turbulence kinetic equation

$$\frac{\partial I_e(k,t)}{\partial t} = 2\psi_e(k,t) I_e(k,t) + S_e(k) - \psi_{\rm LD}(k) I_e(k,t) - \sum_i d_i I_e(k,t) I_i(k,t), \quad (6)$$

where the red terms refer to the quasilinear evolution. The nonred terms describe the steady spontaneous emission coefficient (S_e), the Landau damping ($\psi_{\rm LD}(k)$) of electrostatic waves by the thermal IGM $e-p$-plasma and the nonlinear wave-wave interactions with other eigenmodes (e. g. ion sound waves, transverse filamentation and Weibel modes. . .) of intensity $I_i(k,t)$), including nonlinear Landau damping when $i = e$. The other eigenmodes obey similar kinetic equations.

RUHR-UNIVERSITÄT BOCHUM
Theoretische Physik IV: Weltraum- und Astrophysik

RUB

Pair beam saturation (2)

The electrostatic growth rate is given by

$$\psi_e(k,t) = \frac{\pi^2}{2} \sum_{j=e^+,e^-} \omega_{p,j}^2 \int_{-\infty}^{\infty} dp_\parallel$$

$$\times \int_0^{\infty} dp_\perp \frac{p_\parallel p_\perp}{\gamma} \delta\left(\frac{k p_\parallel}{\gamma m_e} - \omega_R\right) \frac{\partial f_j(p_\parallel, p_\perp, t)}{\partial p_\parallel} \qquad (7)$$

At time $t = 0$ the waves are due to the spontaneous emission of the IGM plasma (its noncollective emission is shown in Fig. 14).

One starts with a beam particle spectrum that is a δ-function in momentum parallel to the ambient magnetic field with $p_\parallel = P = m_e c\sqrt{\Gamma^2 - 1}$. The final state of the evolution of the electrostatic instability is reached at time t_e when both, the growth rate and temporal derivative of the particle distribution function are zero,

RUHR-UNIVERSITÄT BOCHUM
Theoretische Physik IV: Weltraum- und Astrophysik

RUB

Pair beam saturation (3)

i.e. when $\partial f_j/\partial p_\parallel = 0$, which is referred to as the "plateau distribution" (with Heaviside function H), i.e. with $f_j = (2\pi p_\perp)^{-1}\delta(p_\perp)G_j(p_\parallel, t)$

$$G_j(p_\parallel, t=0) = \delta(p_\parallel - P), \quad G_j(p_\parallel, t_e) = \frac{H[P-p_\parallel]H[p_\parallel]}{P} \tag{8}$$

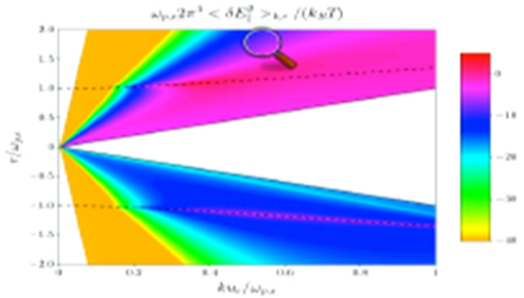

Figure 14: Colour plot in logarithmic powers of e of the spontaneously emitted weakly damped/amplified parallel non-collective electric field fluctuation spectrum in the thermal nonrelativistic $e-p$ IGM plasma of thermal electron velocity $u_e = \sqrt{2k_B T_e/m_e} = 10^{-3}c$. The dotted lines shows the dispersion relation $r = \omega_R(k)$ of the collective electrostatic mode, and the black lines represent the weak damping limit and the high-frequeny limit $\omega_R/k > u_e$. From Felten and RS (2013, PoP 20,082117).

RUHR-UNIVERSITÄT BOCHUM
Theoretische Physik IV: Weltraum- und Astrophysik

RUB

Pair beam saturation (2)

The electrostatic growth rate is given by

$$\psi_e(k,t) = \frac{\pi^2}{2} \sum_{j=e^+,e^-} \omega_{p,j}^2 \int_{-\infty}^{\infty} dp_\parallel$$

$$\times \int_0^{\infty} dp_\perp \frac{p_\parallel p_\perp}{\gamma} \delta\left(\frac{k p_\parallel}{\gamma m_e} - \omega_R\right) \frac{\partial f_j(p_\parallel, p_\perp, t)}{\partial p_\parallel} \qquad (7)$$

At time $t = 0$ the waves are due to the spontaneous emission of the IGM plasma (its noncollective emission is shown in Fig. 14).

One starts with a beam particle spectrum that is a δ-function in momentum parallel to the ambient magnetic field with $p_\parallel = P = m_e c\sqrt{\Gamma^2 - 1}$. The final state of the evolution of the electrostatic instability is reached at time t_e when both, the growth rate and temporal derivative of the particle distribution function are zero,

RUHR-UNIVERSITÄT BOCHUM
Theoretische Physik IV: Weltraum- und Astrophysik

RUB

Pair beam saturation (4)

Integrating the quasilinear Eq. (6) over time gives

$$I_e(k,t) - I_e(k,t=0) = \frac{\pi}{2}\sum_j \omega_{p,j}^2 \int_{-\infty}^{\infty} dp_\parallel$$

$$\times \frac{p_\parallel}{\sqrt{1+(\frac{p_\parallel}{m_e c})^2}}\delta\left(\frac{kp_\parallel}{m_e\sqrt{1+(\frac{p_\parallel}{m_e c})^2}} - \omega_R\right)\int_0^t dt' I(k,t')\frac{\partial G_j(p_\parallel,t')}{\partial p_\parallel} \qquad (9)$$

At the same time the phase space density of the beam particles evolves quasilinearly as (**with the same Cherenkov resonance** $\delta(\omega_R - kv_\parallel)$**!**)

$$\frac{\partial G_j}{\partial t} = \pi e^2 \frac{\partial}{\partial p_\parallel}\left[\int_{-\infty}^{\infty} dk\ I_e(k,t)\delta\left(\omega_R - \frac{kp_\parallel}{m_e\sqrt{1+(\frac{p_\parallel}{m_i c})^2}}\right)\frac{\partial G_j}{\partial p_\parallel}\right] \qquad (10)$$

RUHR-UNIVERSITÄT BOCHUM
Theoretische Physik IV: Weltraum- und Astrophysik

RUB

Pair beam saturation (5)

Performing the k-integral in Eq. (10) with

$$\delta(\omega_R - \frac{k p_\parallel}{m_e\sqrt{1+(\frac{p_\parallel}{m_e c})^2}}) = \frac{m_e\sqrt{1+(\frac{p_\parallel}{m_e c})^2}}{|p_\parallel|}\delta(k - \frac{m_e\omega_R\sqrt{1+(\frac{p_\parallel}{m_e c})^2}}{p_\parallel}) \tag{11}$$

yields

$$\frac{\partial G_j}{\partial t} = \pi e^2 m_e \frac{\partial}{\partial p_\parallel}\left[\frac{\sqrt{1+(\frac{p_\parallel}{m_e c})^2}}{|p_\parallel|}\, I_e(\frac{m_e\omega_R\sqrt{1+(\frac{p_\parallel}{m_e c})^2}}{p_\parallel}, t)\frac{\partial G_j}{\partial p_\parallel}\right], \tag{12}$$

which can be integrated over t and $p_\parallel$, resulting in

RUHR-UNIVERSITÄT BOCHUM
Theoretische Physik IV: Weltraum- und Astrophysik

RUB

Pair beam saturation (6)

$$\int_0^t dt' \, I_e\left(\frac{m_e \omega_R \sqrt{1+(\frac{p}{m_e c})^2}}{p}, t'\right) \frac{\partial G_j(p,t')}{\partial p} =$$

$$\frac{|p|}{\pi e^2 m_e \sqrt{1+(\frac{p}{m_e c})^2}} \int_0^p dp_\parallel \left[G_j(p_\parallel, t) - G_j(p_\parallel, t=0)\right] \qquad (13)$$

Likewise, we perform the $p_\parallel$-integration in the wave equation (9) using

$$\delta\left(\frac{k p_\parallel}{m_e \sqrt{1+(\frac{p_\parallel}{m_e c})^2}} - \omega_R\right) = \frac{m_e}{|k|}\left(\frac{N^2}{N^2-1}\right)^{3/2} \delta\left(p_\parallel - \frac{m_e c \, \mathrm{sgn(N)}}{\sqrt{\mathrm{N}^2-1}}\right), \qquad (14)$$

where $N = ck/\omega_R$ is the index of refraction, to obtain

RUHR-UNIVERSITÄT BOCHUM
Theoretische Physik IV: Weltraum- und Astrophysik

RUB

Pair beam saturation (7)

$$I_e(k,t) - I_e(k,t=0) = \frac{\pi m_e^2 c N^2 \mathrm{sgn(N)}}{2|\mathrm{k}|(\mathrm{N}^2-1)^{3/2}} \sum_j \omega_{p,j}^2$$

$$\times \int_0^t dt' I_e(k,t') \frac{\partial G_j(p_\parallel, t')}{\partial p_\parallel}\Big|_{p_\parallel = \frac{m_e c \mathrm{sgn(N)}}{\sqrt{\mathrm{N}^2-1}}} \qquad (15)$$

We note that precisely the left-hand side of Eq. (13) taken at the value of $p = m_e c \mathrm{sgn(N)}/\sqrt{\mathrm{N}^2-1}$ appears in the wave equation (15), so that

$$\Delta I_e(k,t) = I_e(k,t) - I_e(k,t=0) = \frac{m_e^2 c^2 |N| \mathrm{sgn(N)}}{2|\mathrm{k}|(\mathrm{N}^2-1)^{3/2}} \sum_j \omega_{p,j}^2$$

$$\times \int_0^{m_e c \mathrm{sgn(N)}/\sqrt{\mathrm{N}^2-1}} dp_\parallel [G_j(p_\parallel, t) - G_j(p_\parallel, t=0)] \qquad (16)$$

RUHR-UNIVERSITÄT BOCHUM
Theoretische Physik IV: Weltraum- und Astrophysik

RUB

Pair beam saturation (7)

$$I_e(k,t) - I_e(k,t=0) = \frac{\pi m_e^2 c N^2 \mathrm{sgn(N)}}{2|\mathrm{k}|(\mathrm{N}^2-1)^{3/2}} \sum_j \omega_{p,j}^2$$

$$\times \int_0^t dt' I_e(k,t') \frac{\partial G_j(p_\parallel, t')}{\partial p_\parallel}\Big|_{p_\parallel = \frac{m_e c \mathrm{sgn(N)}}{\sqrt{\mathrm{N}^2-1}}} \qquad (15)$$

We note that precisely the left-hand side of Eq. (13) taken at the value of $p = m_e c \mathrm{sgn(N)}/\sqrt{\mathrm{N}^2-1}$ appears in the wave equation (15), so that

$$\Delta I_e(k,t) = I_e(k,t) - I_e(k,t=0) = \frac{m_e^2 c^2 |N| \mathrm{sgn(N)}}{2|\mathrm{k}|(\mathrm{N}^2-1)^{3/2}} \sum_j \omega_{p,j}^2$$

$$\times \int_0^{m_e c \mathrm{sgn(N)}/\sqrt{\mathrm{N}^2-1}} dp_\parallel [G_j(p_\parallel, t) - G_j(p_\parallel, t=0)] \qquad (16)$$

RUHR-UNIVERSITÄT BOCHUM
Theoretische Physik IV: Weltraum- und Astrophysik

RUB

Self-excited electrostatic turbulence

This **electrostatic quasilinear integral** relates the electrostatic wave spectra and particle distribution functions at any time t to the respective quantities at time $t = 0$.

Inserting the two distribution functions (8) at the beginning ($t = 0$) and at t_e in the quasilinear integral (16) allows us the $p_\parallel$-integration to obtain

$$\mathrm{sgn(N)} \int_0^{\mathrm{m_i c sgn(N)}/\sqrt{\mathrm{N^2-1}}} \mathrm{dp_\parallel [G_j(p_\parallel, t_e) - G_j(p_\parallel, t = 0)]}$$

$$= \frac{H[N]}{\sqrt{N^2-1}\sqrt{\Gamma^2-1}} H[\Gamma - \frac{|N|}{\sqrt{N^2-1}}], \qquad (17)$$

so that the fully developed electrostatic turbulence is

RUHR-UNIVERSITÄT BOCHUM
Theoretische Physik IV: Weltraum- und Astrophysik

RUB

Self-excited electrostatic turbulence (2)

$$\Delta I_e(k,t_e) = \frac{m_e^2 c^2 \sum_{j=e^+,e^-} \omega_{p,j}^2}{2e^2|k|\sqrt{\Gamma^2-1}} \frac{|N|H[N]}{(N^2-1)^2} H[\Gamma - \frac{|N|}{\sqrt{N^2-1}}]$$

$$= \frac{4\pi n_b m_e c^2}{\sqrt{\Gamma^2-1}} \frac{|N|H[N]}{|k|(N^2-1)^2} H[\Gamma - \frac{|N|}{\sqrt{N^2-1}}] \quad (18)$$

with $\sum_{j=e^+,e^-} \omega_{p,j}^2 = 8\pi e^2 n_b/m_e$ for pairs.

The total enhancement in electric field fluctuation power due to the plateauing of the pair distribution function is obtained by integrating Eq. (18) over all wavenumbers k resulting in

$$(\delta E)^2 = \frac{2\pi n_b m_e c^2}{\sqrt{\Gamma^2-1}} [\Gamma\sqrt{\Gamma^2-1} - \frac{1}{2} \ln \frac{\Gamma+\sqrt{\Gamma^2-1}}{\Gamma-\sqrt{\Gamma^2-1}}] \simeq 2\pi\Gamma n_b m_e c^2 \quad (19)$$

RUHR-UNIVERSITÄT BOCHUM
Theoretische Physik IV: Weltraum- und Astrophysik

RUB

Self-excited electrostatic turbulence (4)

Hence the change in the electric field fluctuation energy density is

$$\Delta U_{(\delta E)} = \frac{(\delta E)^2}{8\pi} = \frac{1}{4}\Gamma n_b m_e c^2 \tag{20}$$

Electrostatic waves possess equipartition between electric and velocity fluctuations. so that the total change in fluctuation energy density due to plateauing is

$$\Delta U = 2\Delta U_{(\delta E)} = \frac{1}{2}\Gamma n_b m_e c^2, \tag{21}$$

which is **half of the initial energy density of the pair beam**.

The crucial question now is: how to obtain the plateauing time scale t_e?

RUHR-UNIVERSITÄT BOCHUM
Theoretische Physik IV: Weltraum- und Astrophysik

RUB

Self-excited electrostatic turbulence (5)

Three possible methods:
(1) Numerical solutions of the coupled quasilinear wave and kinetic equations (Grognard 1975, Pavan et al. 2011) indicate for **nonrelativistic** plasmas $t_e \simeq 100 t_E$ where the minimum growth rate $t_E = \psi_{e,\max}^{-1} = 2.8(\Gamma_6/n_{b,-22})^{1/3} n_{e,-7}^{-1/6}$ yrs occurs for oblique fluctuations (RS, Ibscher and Supsar 2012).

(2) An upper limit $t_{e,\max}$ is obtained by assuming that only the guaranteed spontaneous emission of electrostatic waves by the IGM plasma relaxes the particle beam in Eq. (12).

(3) A lower limit $t_{e,\mathrm{low}}$ is obtained by assuming that already at $t = 0$ the fully-developed electrostatic turbulence (18) is available for the relaxation of the particle beam described by Eq. (12).

The true relaxation time scale will be between $t_{e,\mathrm{low}} \leq t_e \leq t_{e,\max}$.

RUHR-UNIVERSITÄT BOCHUM
Theoretische Physik IV: Weltraum- und Astrophysik

RUB

Self-excited electrostatic turbulence (6)

Method (3) provides for the particle kinetic equation (12) with the variable $x = |p_{||}|/m_i c$

$$\frac{\partial G_j}{\partial t} = \frac{\partial}{\partial x}\left[\frac{x^2}{\tau(x)}\frac{\partial G_j}{\partial x}\right] \tag{22}$$

with the relaxation time scale

$$\tau(x) = \frac{\tau_0}{x\sqrt{1+x^2}} \simeq \frac{\tau_0}{x^2} \quad \tau_0 = 2t_0 = \frac{2\sqrt{\Gamma^2-1}}{\pi\omega_{p,e}}\frac{n_e}{n_b} = 1.1\cdot 10^{12}\,\frac{n_{e,-7}^{\frac{1}{2}}\Gamma_6}{n_{b,-22}}\ \text{yrs} \tag{23}$$

for values of $0 \le x \le \sqrt{\Gamma^2-1} \simeq \Gamma$. For momenta $x > 674 n_{e,-7}^{\frac{1}{4}}\Gamma_6 n_{b,-22}^{-\frac{1}{2}}$ the time scale $\tau(x)$ is shorter than the inverse Compton scattering time scale $t_{IC} = 2.5\cdot 10^6 \Gamma_6^{-1}$ yrs.

RUHR-UNIVERSITÄT BOCHUM
Theoretische Physik IV: Weltraum- und Astrophysik

RUB

Self-excited electrostatic turbulence (7)

The kinetic equation (22) for $x \gg 1$ reads

$$\tau_0 \frac{\partial G_j}{\partial t} = \frac{\partial}{\partial x}\left[x^4 \frac{\partial G_j}{\partial x}\right] \tag{24}$$

with the initial condition $G(x,0) = \delta(x - x_0)$, $x_0 = \sqrt{\Gamma^2 - 1}$, has the solution with $T = t/\tau_0 = t/2t_0$

$$G_j(x, x_0, T) = \frac{I_{3/2}\left(\frac{1}{2Tx_0x}\right)}{2T(x_0x)^{3/2}} e^{-\frac{x_0^2+x^2}{4x_0^2x^2T}}$$

$$\simeq \left\{ \begin{array}{ll} \frac{e^{-\frac{1}{4T}\left(\frac{1}{x}-\frac{1}{x_0}\right)^2}}{2x_0x\sqrt{\pi T}} & \text{for } t \gg \frac{t_0}{\Gamma x} \\ \frac{16\,T^{1/2}}{3\pi^{1/2}} e^{-\frac{x_0^2+x^2}{4x_0^2x^2T}} & \text{for } t < \frac{t_0}{\Gamma x} \end{array} \right\} \tag{25}$$

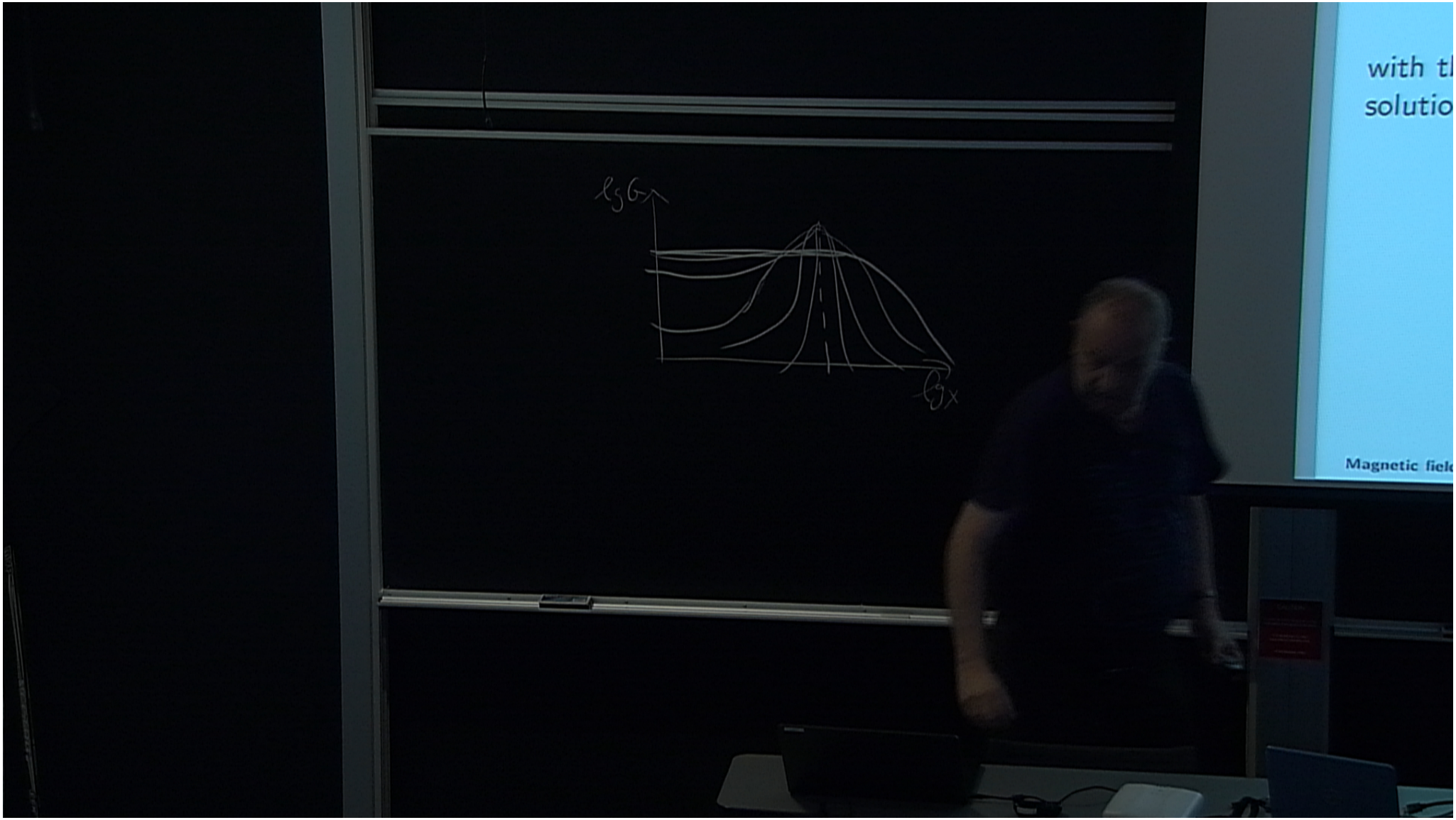
with t
solutio
Magnetic fiel

RUHR-UNIVERSITÄT BOCHUM
Theoretische Physik IV: Weltraum- und Astrophysik

RUB

Beyond the quasilinear approach

One accounts for additional nonquasilinear effects in the kinetic equation (6) by dividing the quasilinear relaxation time scales t_e by a factor $\alpha > 1$, where $\alpha = \psi_E / \psi_{\rm nonlinear}$ (Lesch and RS 1987).

If the nonlinear growth rates are much smaller than ψ_E, the quasilinear relaxation time is prolonged to αt_e which implies the nonlinear stabilization of the beam (RS, Ibscher and Supsar 2012).

Pending: Repeat the quasilinear relaxation analysis for oblique electrostatic waves.

The same analysis , mutattis mutandi, can be applied to relativistic hadron beams (see talk by S. Krakau).